Title:

Differential expression of sex regulatory genes in gonads of *Astyanax mexicanus* surface fish and cavefish

Authors:

Kaitlyn A. Webster[1], Bethany Ponte[2], Hans Vasquez-Gross[3], Juli Petereit[3], John Hutchinson[4], Misty R. Riddle[2*]

Affiliations:

1. Harvard Medical School, Boston, MA, USA
2. University of Nevada, Reno, Reno, Nevada, USA
3. Nevada Bioinformatics Center (RRID:SCR_017802), University of Nevada, Reno, Reno, Nevada, USA
4. Harvard T.H. Chan School of Public Health, Boston, MA, USA

* Corresponding author: mistyriddle@unr.edu

Abstract

Background: *Astyanax mexicanus* is a single species of fish that consists of river-dwelling (surface) and cave-dwelling morphotypes. Little is known about how sexual determination, differentiation or reproduction have evolved in the surface morphs or cavefish, though divergence in reproductive strategy is expected as the latter have adapted to the novel cave environment. Evolution of the gonad transcriptome may underlie the differences in gamete morphology, fertility, and fecundity previously reported between morphotypes.

Results: We compared the ovary and testis transcriptome of surface fish and cavefish at juvenile and adult stages. We found that samples clustered by developmental stage, sex, and morphotype identity. Several key genes that are typically associated with the female gonad in other vertebrates showed a reversal in sexual dimorphism or were not differentially expressed between sexes in *A. mexicanus*. In contrast, while gene expression typically associated with male gonads was largely conserved and consistent with vertebrate testicular expression profiles. Transcriptional and physiological differences between surface fish and cavefish morphotypes were observed in gonads from both sexes. Cavefish ovaries exhibited unique upregulation of neuron development and differentiation genes, and extensive innervation of the ovarian epithelium, while cavefish testes showed increased expression of angiogenesis regulating genes, and greater vasculature density compared to surface fish testes.

Conclusions: These results reveal significant gene expression differences between *A. mexicanus* surface fish and cavefish morphotypes that may have functional consequences in gonad morphogenesis and fertility. Our findings provide a foundation for investigating the evolution of

38 sex regulatory pathways and reproductive strategies in animals adapting to new and challenging
39 environments in which nutrient availability, temperature, and mate selection are suboptimal.
40
41 **Keywords:** *Astyanax mexicanus*, gonad, sex differentiation, transcriptome, ovary, testis, *foxl2*,
42 *cyp19a1a*, teleost
43
44 **Background**
45 Studying gonadal sex differentiation in fishes can help identify novel molecular pathways
46 that mediate sex determination and development. In contrast to mammals, which universally
47 utilize chromosomal XY sex determination directed by the *SOX3*-derived *SRY* gene, fishes display
48 a diversity of sex determining mechanisms (SDM) and sex regulatory genes. Across teleosts,
49 SDM are known to be plastic, rapidly evolving, and inclusive of all known modes of regulation:
50 chromosomal, polygenic, hormonal, social, and environmental (Devlin and Nagahama 2002;
51 Schartl 2004). Different SDM and master sex regulatory genes can evolve even within the same
52 genus, as reported in closely related species of Medaka rice fish (Matsuda 2002, Myosho 2012,
53 Takehana 2014). Like other non-mammalian vertebrates, teleost fish sex determination can be
54 influenced and overridden by social dynamics and environmental conditions, even when sex
55 chromosomes or sex regulatory genes are employed. Notably, environmental factors such as
56 photoperiod, temperature, salinity, pH and hypoxia have been shown to skew sex ratios in
57 teleosts (Brown 2014, Baroiller 2009, Abucay 1999, Shang 2006). Despite the diversity of SDM,
58 most vertebrate sex regulatory genes have orthologues in teleosts, which have been well
59 studied in zebrafish, Medaka, and tilapia. For example, the mammalian ovary-promoting genes

60 *Foxl2*, *Wnt4*, and *Cyp19* (aromatase) show conserved female-specific function in teleosts, as do
61 the testis-promoting genes *dmrt1*, *amh*, and *sox9* (Yang 2017, Kossack 2017, Lau 2016, Guigen
62 2010, Webster 2017, Yan 2019, Nakamura 2012). How sex differentiation and gonad
63 development evolve as fishes adapt to new environments is not well understood.

64 The Mexican tetra, *Astyanax mexicanus,* is a species of fish that consists of river-adapted
65 and cave-adapted morphotypes. There are as many as 32 geographically separate cave-dwelling
66 "cavefish" populations that evolved from river-dwelling "surface fish" in the underground
67 limestone caves of the El Abra Region of Tamaulipas and San Luis Potosí, Mexico (Figure 1D)
68 (Espinasa et al., 2020). Based on whole genome sequencing of field-collected individuals, the *A.*
69 *mexicanus* phylogeny defines two lineages; cavefish from the Tinaja and Pachón caves form a
70 monophyletic clade separate from the Molino cavefish and Río Choy surface fish (Herman et al.,
71 2018). This evolutionary history indicates that cavefish traits have evolved through repeated
72 evolution providing researchers with natural replicates to investigate the genetic and
73 developmental basis of cavefish traits.

74 Little is known about sex and gonad development in *A. mexicanus* despite its growing
75 importance as a model system in understanding the genetic basis of evolution (Perera 2023).
76 For example, only a few studies have compared the expression or function of sex-associated
77 genes between surface fish and cavefish morphs. In Pachón cavefish, sex-associated genes such
78 as *foxl2a*, *wnt4b*, *cyp19a1a*, *dmrt1*, and *amh* were reported to be expressed in the gonads but
79 surprisingly *foxl2a*, *wnt4b*, and *cyp19a1a* were not found to be significantly sexually dimorphic
80 (Imarazene 2021a). Pachón cavefish male sex is determined by supernumerary "B-sex"
81 chromosomes that exhibit non-mendelian inheritance (Imarazene et al., 2021b). The gene

82 conferring male sex on the Pachón cavefish B chromosome is *growth differentiation factor 6b*
83 (*gdf6b*) which if knocked out results in male-to-female sex reversals (Imarazene et al., 2021b).
84 The mechanisms of sex determination in surface fish and other cavefish populations have yet to
85 be described. The atypical expression of conserved vertebrate sex-specific genes and
86 emergence of a novel sex determination mechanism in Pachón cavefish highlights the promise
87 of this model for the study of evolution of sex regulatory pathways and adaptive reproductive
88 strategies. In addition, since traits like body condition and relative organ size are sexually
89 dimorphic and are controlled by loci that have sex-dependent effects (Riddle et al., 2021),
90 revealing how sex determination and gonad development differs between *A. mexicanus*
91 morphs is crucial to understanding cavefish evolution.
92 Here, we describe the first transcriptomic analysis of ovaries and testis in *A. mexicanus,*
93 comparing surface fish and Pachón cavefish at juvenile and adult stages. We found that samples
94 clustered by developmental stage, sex, and morphotype identity. We found that in surface fish
95 and Pachón cavefish, typical female-associated genes are not differentially expressed between
96 males and females. However, typical male-associated gene expression is conserved. We
97 observed an upregulation of genes involved in neuron development in Pachón cavefish ovaries
98 compared to surface fish ovaries and found that the germinal epithelium surrounding germ
99 cells is extensively innervated in both morphotypes. Comparing the testis, we observed
100 increased expression of angiogenesis genes in Pachón cavefish compared to surface fish and
101 evidence of more vasculature within the Pachón cavefish testis. Our results provide insight into
102 the molecular, functional, and structural differences between surface fish and cavefish gonads

103 which is essential for future studies examining the evolution of sex differentiation, sexual

104 dimorphism, and reproduction in this model system.

105

106 **Methods**

107 *Animal husbandry*

108 Río Choy surface fish and Pachón cavefish were derived from parents bred for greater
109 than five generations in the laboratory of Dr. Clifford Tabin at Harvard Medical School. All
110 animals used in this study were maintained, housed, and fed under the same conditions on a
111 recirculating water system (Temperature: 23-24 °C, pH: 7–7.5, Conductivity: 1200-1400µS) in a
112 facility with a 10:14-h light/dark cycle. Adult fish were fed with a combination of New Life
113 Spectrum TheraA+ small and/or medium sinking pellets (dependent on fish size)
114 and *Artemia* and housed at a density equal to two adult fish per liter of water. Hatched larval
115 fish were fed rotifers up to 14 days post fertilization (dpf) in 1-liter cups of fish-ready water, then
116 transferred to the recirculating system where they were fed *Artemia* through 60 dpf. At 1.5
117 years post fertilization, fish were euthanized in MS-222 prior to gonad dissection. We found that
118 adult Pachón cavefish males and females were on average larger than surface fish counterparts
119 with larger gonads, but did not observe significant differences in size between morphotypes
120 (Pachón cavefish versus surface fish average fish weight: male = 1.34g vs 0.95g, p = 0.09, female
121 = 1.9g vs 1.2g, p = 0.17, t-test, Pachón cavefish versus surface fish average gonad weight: testes
122 = 0.034g vs 0.024g, p = 0.40, ovaries = 0.165g vs .097g, p = 0.46, Additional file 1).

123

124 *Sample collection, RNA extraction and cDNA synthesis*

125 Juvenile (i.e., not containing ovulatory eggs or caudal duct spermatozoa) to adult fish aged
126 between 1-1.5 years were euthanized in 400ppm MS-222. The gonads were dissected into cold
127 1 X PBS, and thoroughly cleared of associated fat or viscera using a dissecting microscope.

128 Cleaned gonads were then collected into 0.5mL (adult gonads) or 0.25mL (juvenile gonads)
129 Trizol and homogenized using a hand-held pellet pestle, then stored at −80°C. Total RNA was
130 extracted using Zymo Research Direct-zol RNA MicroPrep with DNAse treatment according to
131 the manufacturers protocol. LunaScript RT Supermix kit with 1µg of RNA was used to synthesize
132 cDNA. Diluted cDNA samples (50ng/µL) were used for sequencing.
133
134 *RNA sequencing and gene ontology analysis*
135 Illumina sequencing was performed by the Nevada Genomics Center using NextSeq 2000 P3 100
136 cycle sequencing kit. Samples were sequenced with 50bp paired-end reads with a mean of 52.2
137 million reads (minimum depth of 29.6 to 58.8 million reads per sample). FastQC v0.11.9 was ran
138 on each sequenced sample both pre and post read trimming to assess improvement after
139 trimming. Trimmomatic v0.36 with parameters ILLUMINACLIP:2:30:10 SLIDINGWINDOW:4:15
140 MINLEN:36 was used in order to remove Illumina sequencing adapters and poor base quality
141 regions.
142 Reads were aligned to Ensembl build 2 of the *A. mexicanus* genome, augmented with transcript
143 information from Ensembl release 2.0.97 using STAR v2.7.5c (Dobin et al., 2013). STAR output
144 alignment BAM files were imported into featureCounts v2.0 from the subread package in order
145 to quantify reads per sample for genes. Quantified counts generated via featureCounts were
146 imported into the statistical software package R (R-core-team, 2019) for downstream analysis. A
147 low count was defined by less than 10 counts per gene. If a gene demonstrated low counts
148 across all samples and experimental groups, it was removed from further downstream analysis.
149 Differential gene analysis was performed with the DESeq2 package (Love 2014) and statistically

150 significant differences were defined by a Benjamini-Hochberg FDR adjusted *p*-value <0.05.

151 Variance stabilizing transformation (VST) was used to visualize count data in a Principal

152 Component Analysis plot.

153 To gain more insight into the differentially expressed genes, gene names were annotated using

154 the biomaRt package (Durinck 2005), and we determined enriched Biological Processes Gene

155 Ontologies (BP GO) using clusterProfiler (Yu 2012). Gene ontology maps were generated from

156 enriched Biological Processes GO terms for differentially expressed genes (padj < 0.05) using

157 clusterProfiler cnetplot function (Yu 2012). Annotation hub AH107459 was used for *Astyanax*

158 *mexicanus* GO term annotation.

159

160 *Ovary immunostaining*

161 Ovaries from adult Pachón cavefish and surface fish were dissected, fixed in 4% PFA, and

162 dehydrated in ethanol. After rehydration, the tissue was incubated with α-acetylated tubulin

163 (1:500, Sigma-Alrich, T6793) in blocking solution (BSA, sodium azide, goat serum, DMSO, PBS,

164 and Triton X-100) for 48 hours at room temperature, rinsed and incubated with a secondary

165 antibody (goat anti-mouse 488 IgG H&L, ABCam, ab150117) for another 48 hours at room

166 temperature. The tissue was imaged on a Leica THUNDER model organism microscope.

167

168 *Testes Vascular Staining and Quantification*

169 Testes were dissected from adult Pachón cavefish and surface fish and collected into 1 x PBS at

170 room temperature, briefly. Whole testes were then immediately incubated for 5 minutes in the

171 dark in a solution of o-Dianisidine (3,3'-dimethoxybenzidine, MilliporeSigma D9143-5G)

172 formulated as described in O'Brien 2009. Stained testes were dehydrated, cleared in xylene, and
173 embedded in paraffin. Sections of 10 uM were then counterstained with modified Harris
174 hematoxylin solution (Sigma-Aldrich HHS32). Tissue area was calculated using ImageJ. Each
175 bundle of vascular staining was traced, and the area was recorded. The vascular area was
176 summed and divided by the total tissue area in the image to calculate percentage of testicular
177 vascularization.
178

179 **Results**

180 We compared the ovary and testes transcriptome of *A. mexicanus* surface fish and
181 Pachón cavefish that were 14-18 months post fertilization (Figure 1 A-E). Interestingly,
182 regardless of chronological age, two distinct morphological stages of gonads were observed for
183 each sex, referred to in this study as juvenile (not containing mature gametes) or adult
184 (containing mature gametes). Gonads categorized as juvenile appeared small and translucent
185 upon dissection, and by histology were confirmed to lack ovulatory oocytes (females) or
186 spermatozoa (males). Adult gonads were large and opaque, and stored mature gametes in the
187 urogenital ducts. Overall, the gonad morphology was similar comparing surface fish and Pachón
188 cavefish, with the most striking difference observed in coloration. Surface testes were sheathed
189 in scattered black melanocytes (Figure 1B), whereas Pachón testes lacked any melanin
190 pigmentation consistent with albinism (Protas 2006) (Figure 1C). Conversely, Pachón cavefish
191 ovaries were intensely yellow-orange compared to surface fish ovaries, consistent with
192 increased carotenoid accumulation in the eggs (Riddle 2020) (Figure 1E).

193 We first visualized transcriptome differences between sample types (n=3 per
194 developmental stage, sex, and morphotype) using principal component analysis and found that
195 samples clustered according to sex and morphotype identity (Figure 1J). We found that PC1
196 (57% variance) separates testes from ovaries, while PC2 (27% variance) separates surface fish
197 from Pachón cavefish. Juvenile and adult gonads formed overlapping clusters except for surface
198 fish ovaries that showed no overlap between developmental stages. These findings indicate
199 differential regulation of gene expression between *A. mexicanus* morphotypes within the
200 gonads of males and females.

201 We examined the gene expression profiles that were specific to each sex to investigate
202 if the function of known regulators of sex differentiation in other species are likely conserved in
203 *A. mexicanus.* We found 17,955 differentially expressed genes (DEG) between the testes and
204 ovaries of *A. mexicanus* (Figure 2A). We observed expected sexually dimorphic expression of
205 some highly conserved and commonly studied sex regulatory genes, but also found that several
206 genes which are customarily restricted to the ovary or upregulated in the ovary, as best
207 characterized in the zebrafish model, are not sexually dimorphic (Figure 2B). For example, the
208 germ-plasm aggregator bucky ball (*buc*) is more highly expressed in the ovary but is also
209 unexpectedly abundant in the testes which do not express *buc* in other teleosts (Figure 2J).
210 Other ovary-associated genes such as the estrogen synthesis enzyme aromatase (*cyp19a1a*),
211 the gonadal somatic cell transcription factor Forkhead box protein L2 (*foxl2a*), and the secreted
212 growth factor wingless-type MMTV integration site family, member 4 (*wnt4a*) were either not
213 sexually dimorphic in the gonads (*cyp19a1a*, Figure 2C), or exhibit a sex-reversed expression
214 profile, i.e. were unexpectedly more highly expressed in the testes (*foxl2a* and *wnt4a*, Figure
215 2D-E). These results suggest possible neofunctionalization of these sex regulators in *A.*
216 *mexicanus*. In contrast to female-promoting genes, male-promoting genes displayed expected
217 patterns of expression comparing ovaries and testes. For example, the TGF-β superfamily
218 member anti-Müllerian hormone (*amh* Figure 2F), the androgen synthesis enzyme Cytochrome
219 P450, family 11 (*cyp11c1*, Figure 2G), the doublesex and mab-3 related transcription factor 1
220 (*dmrt1*, Figure 2H), and the teleost-specific TGF-β superfamily member gonadal soma derived
221 factor (*gsdf*, Figure 2I) were upregulated in the testes of both Pachón cavefish and surface fish.

222 We next compared the ovary transcriptome between surface fish and cavefish
223 morphotypes (Figure 3). Comparing juveniles, we observed 7,312 DEG between morphotypes
224 (Figure 3A). Interestingly, the gene that is most statistically significantly upregulated comparing
225 juvenile Pachón cavefish versus surface fish ovaries was *spock2* (Testican-2), which is a calcium-
226 binding proteoglycan that mediates oocyte maturation in mice. Comparing adults, we found
227 3,698 DEG (Figure 3B). We found that the top 3 gene ontology (GO) term categories for genes
228 upregulated in Pachón juvenile ovaries are protein phosphorylation, neuron development, and
229 plasma membrane bounded cell projection organization (Figure 3C). Similarly, in Pachón adult
230 ovaries the top categories are nervous system development, neuron differentiation, and
231 generation of neurons (Figure 3D). *Semaphorin 3aa* (*sema3aa*) is one of the most upregulated
232 genes in Pachón ovaries of both stages and is implicated in the migration of specialized neurons
233 that secrete gonadotropin-releasing hormone (GnRH) – a critical mediator of puberty and
234 subsequent reproductive cycling (Giacobini 2015). Overall, these findings indicate an
235 upregulation of neuron-associated genes in the ovaries of Pachón cavefish compared to surface
236 fish.
237 In line with a role for neurons in the regulation of ovary function, we observed
238 substantial innervation throughout the sheath that surrounds the ovary, the geminal
239 epithelium, in both morphotypes (Figure 3F-H). A large neuron trunk that branches to reach
240 throughout the ovary germinal epithelium was visible on medial side of the ovary while the
241 lateral side of the ovary shows little to no innervation. A similar innervation pattern is observed
242 in zebrafish and is thought to be important to regulate oocyte quiescence through

243 norepinephrine signaling (Kim 2021). Our findings suggest that altered neuronal signaling may
244 be important for the evolution of cavefish ovaries.
245 We next compared the testes transcriptome between surface fish and cavefish
246 morphotypes (Figure 5). Interestingly, the testes transcriptome was more similar between
247 morphotypes than the ovary transcriptome. We found 1,505 DEG comparing juvenile testes and
248 4,038 DEG comparing adult testes of Pachón cavefish versus surface fish (Figure 4A and 4B,
249 respectively). Many of the most highly expressed DEG in either morph are unannotated, novel
250 genes. However, the most statistically significantly upregulated gene in adult Pachón testes was
251 Syntaxin 5a-like (*stx5al*), which is expressed in mammalian Sertoli cells (somatic nurse cells of
252 the testicular germ cells), but has also been reported as a primordial germ cell marker in
253 zebrafish single-cell RNAseq atlas Daniocell (Sur 2023). Gene set enrichment analysis of the
254 genes upregulated in Pachón testes revealed Biological Process GO term categories related to
255 angiogenesis in juveniles, and cell-cell signaling in adult testes (Figure 4C-D), likely representing
256 morphogenesis/patterning and sperm surface interactants, respectively. Consistent with these
257 gene expression differences, we found that in surface fish testes, blood vessels or vascular
258 bundles were scant, while in Pachón testes most testicular tubules were associated peripherally
259 with vascular tissue (Figure 4D). Our results at the transcriptional and morphological levels,
260 suggest increased vascularization of the cavefish testes which could have an impact on the
261 regulation of spermatogenesis.
262

263

264 **Discussion**

265 In this study, we present the first transcriptomic analysis of ovaries and testes in
266 *Astyanax mexicanus,* comparing gene expression between lab-raised surface fish and Pachón
267 cavefish at both juvenile and adult stages. Our results reveal clustering of samples based on
268 developmental stage, sex, and morphotype identity, demonstrating that these factors play
269 significant roles in shaping gonadal gene expression. This clustering supports the idea that
270 despite the shared ancestry of surface and cave morphotypes, their reproductive systems
271 exhibit distinct developmental trajectories resulting from evolution under different
272 environmental pressures. This transcriptome will enable the identification and characterization
273 of novel and conserved sex-specific genes that drive gonadal sex differentiation in juveniles and
274 maintain sex fate determinations in adults, which in teleost fish requires both male pathway
275 promotion and sustained female pathway suppression (Nishimura and Tanaka 2014). These
276 findings also highlight the potential for *A. mexicanus* to serve as a model for studying the rapid
277 evolution of highly conserved vertebrate sex regulating genes, especially in the context of
278 extreme environmental and nutritional deficits.

279 ***Conservation and deviation in expression profiles of conserved sex genes***

280 Broadly compared to other male vertebrates, our *A. mexicanus* gonadal transcriptome
281 establishes a high degree of conserved gene expression associated with testicular
282 differentiation and spermatogenesis. All male gonad-promoting candidates investigated were
283 expressed uniquely in, or significantly upregulated in testes of both morphotypes, including
284 transcription factors (*dmrt1, sox9a*), signaling molecules (*amh*), and steroidogenic enzymes

285 (*cyp11c1*). These results are consistent with expression profiles reported in other fish testis
286 transcriptomes, and furthermore indicate homology of testicular cell subtypes relative to other
287 vertebrates, including humans (Nynca 2022, Qian 2022, Liu 2023). However, despite typical
288 expression of testis-enriched transcripts, our data show a striking deviation from other fishes or
289 vertebrates with respect to the expression of canonically ovary-promoting genes. This suggests
290 possible evolution, differential selection, or neofunctionalization of ovarian genes in *A.*
291 *mexicanus*.

292 Most strikingly, we identified a reversal of sexually dimorphic expression in *foxl2a*, an
293 evolutionarily conserved transcription factor produced by somatic cells of the differentiating
294 ovary in all metazoans. Across species, *foxl2a/*Foxl2a is typically an ovary-enriched transcript
295 and protein. Transcript levels of *foxl2a* will not necessarily correlate to protein products active
296 in the testis, however, highlighting the importance of further experiments. Foxl2 has a
297 complicated history of repeated gains, losses, and role changing, but generally is present in fish
298 genomes as *foxl2a* or *foxl2b*, with some basal teleosts retaining both *foxl2a* and *foxl2b* (Bertho
299 2016). We identified *foxl2a*, *foxl2b*, and the paralog *foxl3* in the *A. mexicanus* ovary and testis
300 transcriptomes. Surprisingly, our data show that *foxl2b* is more highly expressed in ovaries than
301 testes, despite its sequence being highly divergent from other teleosts exhibiting male-enriched
302 or non-dimorphic expression of this gene. While *A. mexicanus foxl2a* shows 75-80% identity to
303 its teleost orthologs, there are no known studies reporting higher testicular expression of *foxl2a*
304 in any other fishes, with most reporting low to no expression in testes (summarized in Bertho
305 2016). High expression of *FOXL2* protein has, however, been reported in American alligator
306 testes prior to temperature-dependent sex determination (Yatsu 2016), which may point to

307 latent sexual plasticity of the *A. mexicanus* testis. Taken together, it is possible that
308 neofunctionalization – or impairment of functionalization – of *foxl2a* in *A. mexicanus* has
309 conferred a novel role upon this gene in the testis, while *foxl2b* has retained an ovary-
310 promoting function.

311 Downstream of ovary-promoting transcription factors such as *foxl2a*, expression of the
312 steroidogenic enzyme aromatase (*cyp19a1a*) typically signals ovarian differentiation and
313 commitment in vertebrates via production of feminizing estradiol (E2). We found both
314 morphotypes to lack sexually dimorphic expression of this gene, suggesting deviation from
315 typical sex hormone signaling in *A. mexicanus* and possible elevation of E2 in males. *cyp19a1a* is
316 detected in somatic gonadal cells of both sexes, though in fish is broadly ovary-enriched and in
317 zebrafish is required to antagonize testis fate (Devlin and Nagahama 2002, Dranow 2016).
318 *cyp19a1a* can synthesize E2 through two biochemical pathways, a direct pathway that produces
319 E2 using testosterone produced by the steroidogenic enzyme *hsd17b3*, and an indirect pathway
320 that produces an estrone (E1) intermediate from androstenedione, requiring the action of
321 *hsd17b1* to ultimately generate E2 (Miller and Auchus 2011). Our analysis revealed sexually
322 dimorphic expression of both *hsd17b1* and *hsd17b3* (upregulated in ovaries and testes,
323 respectively), indicating that the deployment of either E2 synthesis pathway 1) differs between
324 sexes and 2) may ultimately result in expected rates or physiological concentrations of sex
325 hormones. The *hsd17b1* E2 synthesis pathway is also favored in zebrafish ovaries, though has
326 not been explored in testes, in which *cyp19a1a* expression is very low and dispensable (Liu
327 2022, Dranow 2016). Future studies of circulating serum hormone levels will be necessary to
328 demonstrate whether *A. mexicanus* males exhibit physiologic aberrantly high estrogen

329 signaling. It is also possible that male *A. mexicanus* produce an inactive *cyp19a1a* protein due
330 to alternative splicing, as reported in the protandrous hermaphrodite barramundi (Domingos
331 2018).

332 ***Upregulation of innervation in cavefish ovaries***

333 Enrichment analysis of the DEGs upregulated in the ovaries of Pachón cavefish versus
334 surface fish suggest possible differences in ovarian physiology. Most notably, we identified
335 enrichment of genes involved in neuron and axon differentiation and development. This is
336 consistent with our observation that the external ovarian epithelium is extensively innervated
337 in both morphotypes (Figure 4). In zebrafish, the ovarian epithelium demarcates a germinal
338 zone that is associated with nests of presumptive germline stem cells (Liu 2022). In the
339 mammalian ovary, nerve cells are connected to the follicles as well as gonadal blood vessels
340 (Malamed 2012), and neurotrophic growth factors and receptors are expressed at varying levels
341 dependent on oocyte stage (reviewed in Linher-Melville and Li 2013). Given this evidence that
342 innervation and neurotrophins influence folliculogenesis and oocyte maturation, enhanced
343 neurogenesis in Pachón ovaries may represent an adaptive reproductive strategy that regulates
344 renewal versus differentiation of ovarian germ cells in the cave environment, which is
345 reproductively challenging both in terms of nutrient deprivation and mate selection.

346 Additionally, increased innervation may facilitate reproductive success in caves in the
347 absence of visual stimuli, by integrating other sensory inputs from the environment that serve
348 as cues for spawning (e.g. temperature, water currents, precipitation). In zebrafish, production
349 of norepinephrine within neurons of the ovary is important for regulating oocyte maturation in
350 response to nutrient cues (Kim 2021). Increased sensitivity to such cues may provide cavefish

351 females an energy-saving advantage as nutrient availability fluctuates seasonally (Espinasa
352 2017). The functional significance of ovarian innervation in cavefish remains speculative, but
353 further studies comparing oocyte development between morphotypes may elucidate how cave
354 environments influence reproductive physiology.

355 ***Upregulation of vascularization in cavefish testes***

356 Enrichment analysis uncovered a striking upregulation in the expression of angiogenesis-
357 related genes in Pachón cavefish compared to surface fish. This molecular evidence is
358 supported by our histological findings of increased vasculature in Pachón cavefish testes (Figure
359 6). Vertebrate seminiferous tubules are typically avascular and form a blood-testis barrier that
360 occludes the germinal epithelium (spermatogonia, spermatocytes, sperm, and Sertoli support
361 cells), though specialized non-fenestrated capillaries form in the interstitial space outside of the
362 seminiferous tubules where the steroidogenic Leydig cells reside (Ergün 2016). In mammals,
363 upregulation of vascularization is necessary for initiating organogenesis of the testis, in
364 particular ensuring development of fetal testis cords and limiting differentiation of the Leydig
365 cell population (reviewed in Gu 2021). Thus, cavefish testicular vascularization may indicate a
366 delayed or repressed state, with respect to sexual maturation. Across species, testes
367 vascularization allows for thermoregulation, establishing optimal timing and temperature for
368 spermiogenesis (Setchell 1998). In many fishes, temperature fluctuation in either direction
369 lowers testosterone production and inhibits germ cell differentiation (Manning and Kime 1985,
370 Konkal and Ganesh 2021). Testicular thermoregulation may be particularly challenging in
371 chronically low-temperature cave environments, and the temperature preferences exhibited by
372 cavefish could represent a reproductive strategy that preserves male fertility (Tabin 2018).

373 Cave environments are also hypoxic, a condition known to induce angiogenesis and
374 vascular branching via upregulated Notch signaling (Krock 2011). Pachón cavefish have adapted
375 to hypoxia by developing more erythrocytes and enlarged hematopoietic domains, driven by an
376 increase in Sonic hedgehog (*shh*) (van der Weele 2024). These studies align with our findings,
377 which show upregulation of *notch1b*, *notch3*, and *shh* specifically in the Pachón testes
378 (Additional file 2). Further comparative analysis of surface and cavefish testes will be needed to
379 characterize differences in rate of spermatogenesis or time to sexual maturity. Our study
380 provides molecular evidence for gonadal adaptation that allows for morphogenesis and
381 spermiogenesis to proceed in the extremes of cave environments.
382
383 **Conclusions**
384 Our study provides new insights into the molecular, functional, and structural
385 differences between surface fish and cavefish gonads, gametes, and fertility, contributing to the
386 broader understanding of reproductive biology in *A. mexicanus*. Reversal or loss of sex-specific
387 gene expression (*foxl2a, cyp19a1a*) suggests novel functional changes or plasticity emerging in
388 conserved sex regulating pathways in this species. The upregulation of neuron development in
389 ovaries and increased angiogenesis in testes highlight the potential for adaptive changes in
390 gonadal tissue architecture and function in response to environmental pressures in the cave.
391 These findings open several avenues for future research, including functional studies to
392 determine how these molecular changes impact reproductive success and how environmental
393 factors shape the evolution of sexual dimorphism and reproduction in cave-adapted

394 populations. Overall, our results establish a foundation for further investigations into the

395 evolution of sex-regulatory pathways and sexual dimorphism in organisms in extreme habitats.

396

397

398

399

400

401 **Declarations**

402 *Ethics approval and consent to participate*

403 This research was performed in compliance with ethical guidelines mandated by Harvard
404 Medical School IACUC (Institutional Animal Care and Use Committee). All fish husbandry,
405 euthanasia, and experimental procedures were conducted according to protocols approved
406 by IACUC and veterinary staff (IACUC Protocol IS00001612-6 [previously identified as
407 #04174], valid through 2026). Fish were humanely euthanized by immersion in a lethal dose
408 (400 ppm) of tricaine (MS-222) dissolved in their environmental water, according to the
409 approved IACUC protocol.

410 *Consent for publication*

411 Not applicable

412

413 *Availability of data and materials*

414 The RNA sequencing datasets generated and analyzed during the current study are available
415 in the NCBI SRA repository (Accession: PRJNA1202205 [Reviewer link:
416 https://dataview.ncbi.nlm.nih.gov/object/PRJNA1202205?reviewer=cecqungnrd9j6h5njki7u7ns
417 hh])

418

419 *Competing interests*

420 The authors declare that they have no competing interests.

Funding

This project was supported by grants from the National Institute of General Medical Sciences (GM103440 and 5 U54 GM104944).

Authors' contributions

KW conceived the study, collected samples, analyzed data, and wrote and edited manuscript draft. BP collected samples, analyzed data, and edited the manuscript draft. HVG, JP, and JH processed and analyzed RNAseq data, and edited the manuscript draft. MR conceived the study, analyzed data, and wrote and edited manuscript draft.

Acknowledgements

Brian Martineau, Emma Ferrante, and Taylor Rebbe provided fish husbandry in the aquatic facility of Clifford J. Tabin at Harvard Medical School.

References

1. Abucay, J., Mair, J., Skibinski, D. & Beardmore, J. Environmental sex determination: the effect of temperature and salinity on sex ratio in *Oreochromis niloticus*. *Aquaculture* 173, 219–234 (1999).

2. Baroiller, J. F., D'Cotta, H. & Saillant, E. Environmental Effects on Fish Sex Determination and Differentiation. *Sexual Development* 3, 118–135 (2009).

3. Bertho, S. *et al.* Foxl2 and Its Relatives Are Evolutionary Conserved Players in Gonadal Sex Differentiation. *Sexual Development* 10, 111–129 (2016).

4. Brown, E. E., Baumann, H. & Conover, D. O. Temperature and photoperiod effects on sex determination in a fish. *Journal of Experimental Marine Biology and Ecology* 461, 39–43 (2014).

5. Devlin, R. H. & Nagahama, Y. Sex determination and sex differentiation in fish: an overview of genetic, physiological, and environmental influences. *Aquaculture* 208, 191–364 (2002).

6. Domingos, J. A. *et al.* Sex-specific *dmrt1* and *cyp19a1* methylation and alternative splicing in gonads of the protandrous hermaphrodite barramundi. *PLOS ONE* 13, e0204182 (2018).

7. Dranow, D. B. *et al.* Bmp15 Is an Oocyte-Produced Signal Required for Maintenance of the Adult Female Sexual Phenotype in Zebrafish. *PLOS Genetics* 12, e1006323 (2016).

8. Durinck, S. *et al.* BioMart and Bioconductor: a powerful link between biological databases and microarray data analysis. *Bioinformatics* 21, 3439–3440 (2005).

9. Elliott, W. R. Cave Exploration and Mapping in the Sierra de El Abra Region. in *Biology and Evolution of the Mexican Cavefish* 9–40 (Elsevier, 2016). doi:10.1016/B978-0-12-802148-4.00001-3.

10. Ergün, S., Davidoff, M. & Holstein, A. F. Capillaries in the lamina propria of human seminiferous tubules are partly fenestrated. *Cell and Tissue Research* 286, 93–102 (1996).

11. Espinasa, L. *et al.* Discovery of Two New *Astyanax* Cavefish Localities Leads to Further Understanding of the Species Biogeography. *Diversity* 12, 368 (2020).

12. Espinasa, L. *et al.* Contrasting feeding habits of post-larval and adult *Astyanax* cavefish. *Subterranean Biology* 21, 1–17 (2017).

463 13. Giacobini, P. Shaping the Reproductive System: Role of Semaphorins in Gonadotropin-
464 Releasing Hormone Development and Function. *Neuroendocrinology* 102, 200–215 (2015).
465 14. Gu, X., Li, S. & DeFalco, T. Immune and vascular contributions to organogenesis of the testis
466 and ovary. *The FEBS Journal* 289, 2386–2408 (2022).
467 15. Guiguen, Y., Fostier, A., Piferrer, F. & Chang, C. F. Ovarian aromatase and estrogens: A pivotal
468 role for gonadal sex differentiation and sex change in fish. *General and Comparative*
469 *Endocrinology* 165, 352–366 (2010).
470 16. Herman, A. *et al.* The role of gene flow in rapid and repeated evolution of cave-related traits
471 in Mexican tetra, Astyanax mexicanus. *Molecular Ecology* 27, 4397–4416 (2018).
472 17. Imarazene, B. *et al.* Primordial Germ Cell Migration and Histological and Molecular
473 Characterization of Gonadal Differentiation in Pachón Cavefish *Astyanax mexicanus*; *Sexual*
474 *Development* **14**, 80–98 (2020).
475 18. Imarazene, B. *et al. A supernumerary "B-sex" chromosome drives male sex 1 determination*
476 *in the Pachón cavefish, Astyanax mexicanus 2 3*. https://ssrn.com/abstract=3875774.
477 19. Kim, J., Hyun, M., Hibi, M. & You, Y. J. Maintenance of quiescent oocytes by noradrenergic
478 signals. *Nature Communications* 12, (2021).
479 **20.** Konkal, P. & Ganesh, C. B. The effect of high or low temperature on testicular activity in the
480 cichlid fish *Oreochromis mossambicus*. *Fisheries Science* 87, 837–844 (2021).
481 21. Kossack, M. E. *et al.* Female Sex Development and Reproductive Duct Formation Depend on
482 Wnt4a in Zebrafish. *Genetics* 211, 219–233 (2019).
483 22. Krock, B. L., Skuli, N. & Simon, M. C. Hypoxia-Induced Angiogenesis: Good and Evil. *Genes &*
484 *Cancer* 2, 1117–1133 (2011).

485 23. Lau, E. S.-W., Zhang, Z., Qin, M. & Ge, W. Knockout of Zebrafish Ovarian Aromatase Gene
486 (cyp19a1a) by TALEN and CRISPR/Cas9 Leads to All-male Offspring Due to Failed Ovarian
487 Differentiation. *Scientific Reports* 6, 37357 (2016).
488 24. Li, F. *et al.* Gonadal Transcriptome Sequencing Analysis Reveals the Candidate Sex-Related
489 Genes and Signaling Pathways in the East Asian Common Octopus, *Octopus sinensis*. *Genes* 15,
490 (2024).
491 25. Linher-Melville, K. & Li, J. The roles of glial cell line-derived neurotrophic factor, brain-
492 derived neurotrophic factor and nerve growth factor during the final stage of folliculogenesis: a
493 focus on oocyte maturation. *REPRODUCTION* 145, R43–R54 (2013).
494 26. Liu, Y. *et al.* Single-cell transcriptome reveals insights into the development and function of
495 the zebrafish ovary. *eLife* **11**, (2022).
496 27. Love, M. I., Huber, W. & Anders, S. Moderated estimation of fold change and dispersion for
497 RNA-seq data with DESeq2. *Genome Biology* 15, 550 (2014).
498 28. Malamed, S., Gibney, J. A. & Ojeda, S. R. Ovarian innervation develops before initiation of
499 folliculogenesis in the rat. *Cell & Tissue Research* 270, 87–93 (1992).
500 29. Manning, N. J. & Kime, D. E. The effect of temperature on testicular steroid production in the
501 rainbow trout, *Salmo gairdneri*, *in vivo* and *in vitro*. *General and Comparative Endocrinology* 57,
502 377–382 (1985).
503 30. Matsuda, M. *et al.* DMY is a Y-specific DM-domain gene required for male development in
504 the medaka fish. *Nature* 417, 559–563 (2002).
505 31. Miller, W. L. & Auchus, R. J. The Molecular Biology, Biochemistry, and Physiology of Human
506 Steroidogenesis and Its Disorders. *Endocrine Reviews* 32, 81–151 (2011).

507 32. Myosho, T. *et al.* Tracing the emergence of a novel sex-determining gene in medaka, *Oryzias*
508 *luzonensis*. *Genetics* 191, 163–170 (2012).
509 33. Nakamura, Y. *et al.* Sox9 Is Upstream of MicroRNA-140 in Cartilage. *Applied Biochemistry*
510 *and Biotechnology* 166, 64–71 (2012).
511 34. Nishimura, T. & Tanaka, M. Gonadal development in fish. *Sexual Development* 8, 252–261
512 (2014).
513 35. Nynca, J. *et al.* Ovarian transcriptome analysis of diploid and triploid rainbow trout revealed
514 new pathways related to gonadal development and fertility. *Animal* 16, 100594 (2022).
515 36. O'Brien, B. Identification of Haemoglobin by its Catalase Reaction with Peroxide and *o* -
516 Dianisidine. *Stain Technology* **36**, 57–61 (1961).
517 37. Perera, P., Perez Guerra, D. & Riddle, M. R. The Mexican Tetra, *Astyanax mexicanus*, as a
518 Model System in Cell and Developmental Biology. *Annual Review of Cell and Developmental*
519 *Biology* **39**, 23–44 (2023).
520 38. Protas, M. E. *et al.* Genetic analysis of cavefish reveals molecular convergence in the
521 evolution of albinism. *Nature Genetics* 38, 107–111 (2006).
522 39. Qian, P., Kang, J., Liu, D. & Xie, G. Single Cell Transcriptome Sequencing of Zebrafish Testis
523 Revealed Novel Spermatogenesis Marker Genes and Stronger Leydig-Germ Cell Paracrine
524 Interactions. *Frontiers in Genetics* 13, (2022).
525 40. Riddle, M. R. *et al.* Genetic architecture underlying changes in carotenoid accumulation
526 during the evolution of the blind Mexican cavefish, *Astyanax mexicanus*. *Journal of Experimental*
527 *Zoology Part B: Molecular and Developmental Evolution* 334, 405–422 (2020).

528 41. Riddle, M. R. *et al.* Genetic mapping of metabolic traits in the blind Mexican cavefish reveals
529 sex-dependent quantitative trait loci associated with cave adaptation. *BMC Ecology and*
530 *Evolution* 21, 94 (2021).
531 42. Schartl, M. Sex chromosome evolution in non-mammalian vertebrates. *Current Opinion in*
532 *Genetics and Development* vol. 14 634–641 at https://doi.org/10.1016/j.gde.2004.09.005
533 (2004).
534 43. Setchell, B. P. The Parkes Lecture Heat and the testis. *Reproduction* 114, 179–194 (1998).
535 44. Shang, E., Yu, R. M. K. & Wu, R. S. S. Hypoxia Affects Sex Differentiation and Development,
536 Leading to a Male-Dominated Population in Zebrafish (*Danio rerio*). *Environmental Science &*
537 *Technology* 40, 3118–3122 (2006).
538 45. Sur A, Wang Y, Capar P, Margolin G, Prochaska MK, Farrell JA. Single-cell analysis of shared
539 signatures and transcriptional diversity during zebrafish development. Dev Cell. 2023 Dec
540 18;58(24):3028-3047.e12. https://daniocell.nichd.nih.gov/gene/S/stx5al/stx5al_pgc.html
541 46. Tabin, J. A. *et al.* Temperature preference of cave and surface populations of Astyanax
542 mexicanus. *Developmental Biology* 441, 338–344 (2018).
543 47. Takehana, Y. *et al.* Co-option of *Sox3* as the male-determining factor on the Y chromosome
544 in the fish *Oryzias dancena*. *Nature Communications* 5, (2014).
545 48. van der Weele, C. M., Hospes, K. C., Rowe, K. E. & Jeffery, W. R. Hypoxia-sonic hedgehog axis
546 as a driver of primitive hematopoiesis development and evolution in cavefish. *Developmental*
547 *Biology* 516, 138–147 (2024).
548 49. Webster, K. A. *et al.* Dmrt1 is necessary for male sexual development in zebrafish.
549 *Developmental Biology* 422, 33–46 (2017).

550 50. Wilson, E. J., Tobler, M., Riesch, R., Martínez-García, L. & García-De León, F. J. Natural history
551 and trophic ecology of three populations of the Mexican cavefish, Astyanax mexicanus.
552 *Environmental Biology of Fishes* 104, 1461–1474 (2021).
553 51. Wu, Y. *et al.* Syntaxin binding protein 2 in Sertoli cells regulates spermatogonial stem cell
554 maintenance through directly interacting with connexin 43 in the testes of neonatal mice.
555 *Molecular Biology Reports* 49, 7557–7566 (2022).
556 52. Yan, Y.L. *et al.* A Hormone That Lost Its Receptor: Anti-Müllerian Hormone (AMH) in
557 Zebrafish Gonad Development and Sex Determination. *Genetics* 213, 529–553 (2019).
558 53. Yang, Y. J., Wang, Y., Li, Z., Zhou, L. & Gui, J. F. Sequential, divergent, and cooperative
559 requirements of *foxl2a* and *foxl2b* in ovary development and maintenance of zebrafish. *Genetics*
560 205, 1551–1572 (2017).
561 54. Yatsu, R. *et al.* RNA-seq analysis of the gonadal transcriptome during *Alligator*
562 *mississippiensis* temperature-dependent sex determination and differentiation. *BMC Genomics*
563 17, 77 (2016).
564 55. Yu, G., Wang, L. G., Han, Y. & He, Q. Y. ClusterProfiler: An R package for comparing biological
565 themes among gene clusters. *OMICS A Journal of Integrative Biology* 16, 284–287 (2012).
566

567 **Figure Legends**

568 **Figure 1. Transcriptome analysis of *Astyanax mexicanus* gonads.** Appearance of *A. mexicanus*
569 surface fish (**A**) and Pachón cavefish (**B**) males and females. Appearance of sexually mature
570 testis and ovaries of surface fish (**C, E**) and Pachón cavefish (**D, F**). Testes (**C, D**) consist of two
571 lobes of tubules containing male germ cells and sperm and terminating at the efferent

572 urogenital duct (white arrowheads). Ovaries (**E-F**) consist of two lobes containing clusters of
573 female germ cells and eggs surrounded by the germinal epithelium and terminating at the
574 oviduct (black arrowhead). (**G**) Principal component analysis (PCA) plot of normalized, variance
575 stabilized RNA sequencing expression profiles of *A. mexicanus* gonads. Each point represents an
576 individual sample, colored by sample type. The first principal component (PC1) explains 57% of
577 the total variance and separates samples by sex. The second principal component (PC2) explains
578 27% of the total variance and separates samples by morphotype (surface fish vs Pachón
579 cavefish). PCA plots based on differentially expressed genes (DEG) only (adjusted p-value less
580 than 0.05).
581
582 **Figure 2. Sex-specific gene expression profiles in *Astyanax mexicanus* surface fish and Pachón**
583 **cavefish gonads.** (**A**) Volcano plot showing genes that are differentially expressed between *A.*
584 *mexicanus* testes and ovaries (includes data from juvenile, adult, surface fish, and Pachón
585 cavefish gonads). The y-axis shows -log10 adjusted p-value and the x-axis shows log2 fold
586 change for all genes after low-count filtering (23,809 transcripts). Genes with adjusted p-value <
587 0.05 and absolute log2 fold change > 1 are highlighted in red. Negative fold change indicates
588 testis-enriched expression, while positive fold change indicates ovary-enriched expression. (**B**)
589 Summary of genes with sex-specific expression profiles in the gonads of zebrafish (*Danio rerio*),
590 compared to the expression profiles we observed in *A. mexicanus.* "Ovary" indicates a gene
591 with upregulation in female gonads, whereas "testis" indicates a gene with upregulation in male
592 gonads. (**C-J**) Plots showing *A. mexicanus* gonad log2 transcript abundance of genes with sex-
593 specific expression profiles and functions in the gonads of other vertebrates. Each point

594 represents the transcript abundance in an individual sample, colored and organized on the x-
595 axis by the sample type. From left to right: cavefish (CF) juvenile ovary, CF adult ovary, surface
596 fish (SF) juvenile ovary, SF adult ovary.
597
598 **Figure 3. Ovary transcriptome differences between surface fish and Pachón cavefish suggest**
599 **enhanced neurogenesis in cavefish.** (**A, B**) Volcano plots showing genes that are differentially
600 expressed between the ovaries of *A. mexicanus* surface fish and Pachón cavefish at juvenile (**A**)
601 and adult (**B**) stages. The y-axis shows -log10 adjusted p-value and the x-axis shows log2 fold
602 change for all genes after low-count filtering. Genes with adjusted p-value < 0.05 and absolute
603 log2 fold change > 1 are highlighted in green. Negative fold change indicates greater expression
604 in surface fish, while positive fold change indicates greater expression in cavefish. (**C**, **D**) Dot
605 plots displaying top 15 enriched biological process gene ontology (GO) terms identified from
606 gene set enrichment analysis of genes upregulated in Pachón cavefish compared to surface fish
607 at juvenile (**C**) and adult (**D**) stages. Each dot represents a biological process GO category, with
608 the size of the dot corresponding to the number of genes in the category, and the color scale
609 indicating the adjusted p-value. The x-axis represents the gene ratio (proportion of input genes
610 involved in the pathway), while the y-axis lists the enriched pathways.
611
612 **Figure 4. Innervation in the *Astyanax mexicanus* ovarian epithelium revealed by wholemount**
613 **immunostaining**. Brightfield images of the ovaries of adult surface fish (**A**) and Pachón cavefish
614 (**B**). Lobes on the lefthand side of the image are placed with the medial side upward, while lobes
615 on the righthand side are placed with the lateral side upward. Visualization of acetylated tubulin

616 in wholemount fluorescence images of the ovaries shown in A, B at low magnification (**B, F**) and
617 higher magnification (**C, D, G, H**) highlighting the differences in innervation in the medial side (**C,**
618 **G**) versus lateral side (**D, H**) of the ovary. A large neuron trunk (solid arrows) can be seen on the
619 medial side of the ovary with branches (dashed arrows) that reach throughout the ovarian
620 epithelium.
621
622 **Figure 5. Testis transcriptome differences between surface fish and Pachón cavefish suggests**
623 **enhanced angiogenesis in cavefish.** (**A,B**) Volcano plots showing genes that are differentially
624 expressed between the testes of *A. mexicanus* surface fish and Pachón cavefish at juvenile (**A**)
625 and adult (**B**) stages. The y-axis shows -log10 adjusted p-value and the x-axis shows log2 fold
626 change for all genes after low-count filtering. Genes with adjusted p-value < 0.05 and absolute
627 log2 fold change > 1 are highlighted in green. Negative fold change indicates greater expression
628 in surface fish, while positive fold change indicates greater expression in cavefish. (**C**, **D**) Dot
629 plots displaying top 15 enriched biological process gene ontology (GO) terms identified from
630 gene set enrichment analysis of genes upregulated in Pachón cavefish compared to surface fish
631 at juvenile (**C**) and adult (**D**) stages. Each dot represents a biological process GO category, with
632 the size of the dot corresponding to the number of genes in the category, and the color scale
633 indicating the adjusted p-value. The x-axis represents the gene ratio (proportion of input genes
634 involved in the pathway), while the y-axis lists the enriched pathways.
635
636 **Figure 6. Histological comparison of testis vasculature between *Astyanax mexicanus* surface**
637 **fish and cavefish.** Histological sections of adult testes stained to visualize blood vessels in

surface fish (A) and Pachón cavefish (B). Vasculature is stained using o-dianisidine (brown) with hematoxylin (blue) as a counterstain. Surface fish testis section (B) shows many seminiferous tubules and only a single vascular bundle (black arrow). In contrast, cavefish testis section shows numerous vascular bundles around the seminiferous tubules (black arrows). se = seminiferous epithelium; sz = spermatozoa.

Additional material

Additional file 1.pptx Boxplots displaying weight of fish (A-B) and gonad (C-D) for the samples used for RNAseq analysis. Juvenile gonads were too small to accurately measure weight. In boxplots central line represents median, upper and lower edges indicate first and third quartiles, and whiskers extend to 1.5 times the interquartile range. No significant differences were observed between sample types (t-test $p > 0.05$).

Additional file 2.pptx Plots showing *A. mexicanus* gonad log2 transcript abundance of genes potentially involved in steroidogenesis (*hsd17b1* and *hsdb17b3*) or vascularization and angiogenesis (*notch1b, notch3, shh*). Each point represents the transcript abundance in an individual sample, colored and organized on the x-axis by the sample type. From left to right: cavefish (CF) juvenile ovary, CF adult ovary, surface fish (SF) juvenile ovary, SF adult ovary.

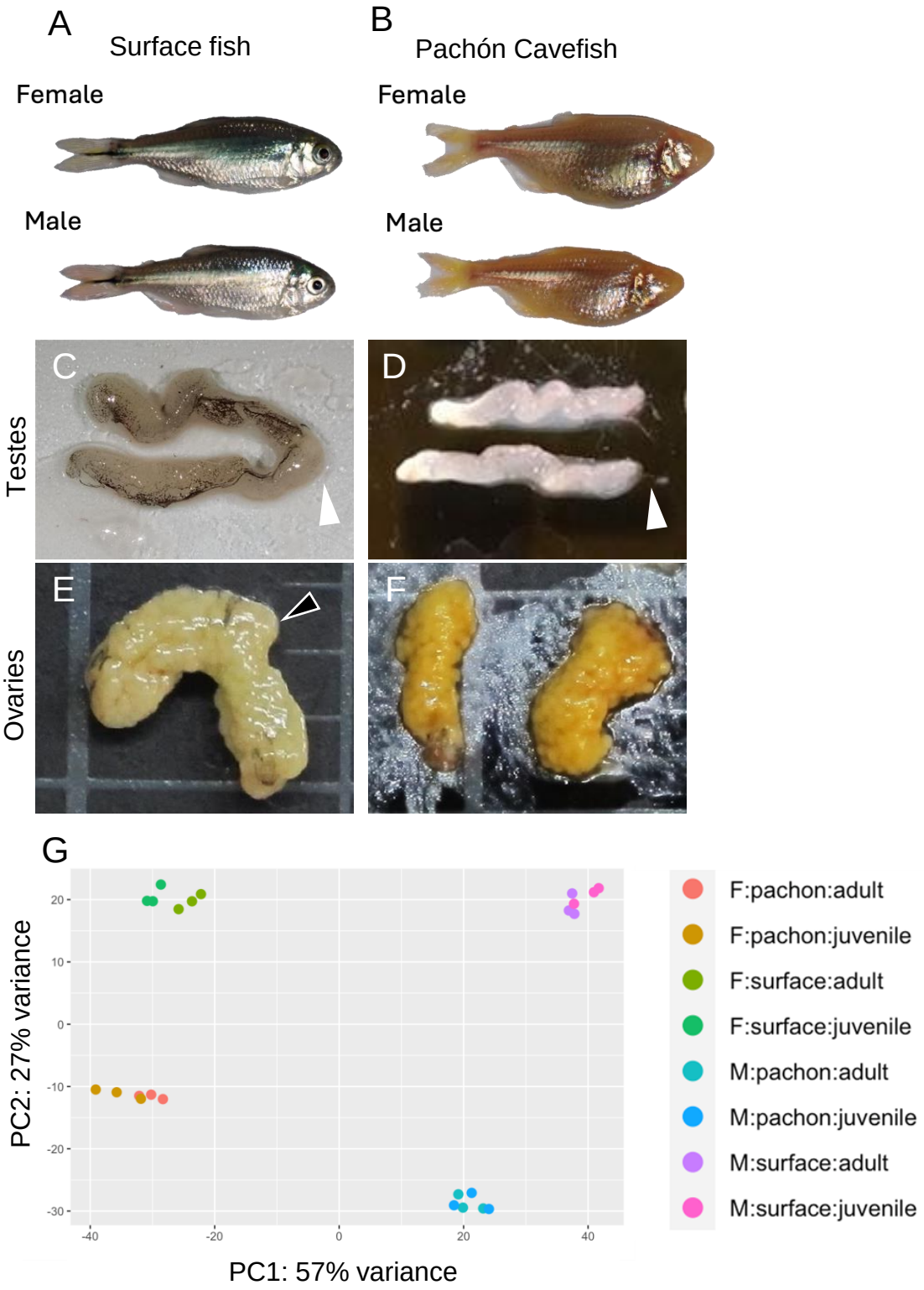
A
Surface fish
B
Pachón Cavefish
Female
Male
Female
Male
C
D
Testes
E
F
Ovaries
G
PC2: 27% variance
PC1: 57% variance
20
10
0
-10
-20
-30
-40
-20
0
20
40
F:pachon:adult
F:pachon:juvenile
F:surface:adult
F:surface:juvenile
M:pachon:adult
M:pachon:juvenile
M:surface:adult
M:surface:juvenile

Figure 1

A

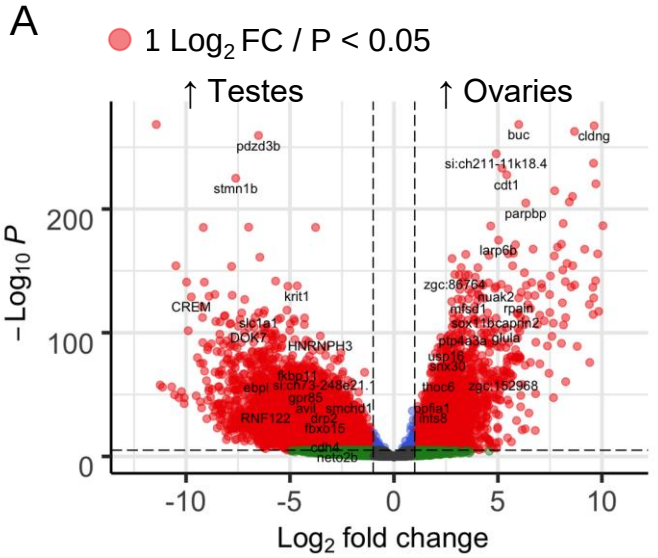

B

Gene	*Danio rerio*	*Astyanax mexicanus*
amh	testis	testis
cyp11c1	testis	testis
cyp19a1a	ovary	not dimorphic
dmrt1	testis	testis
foxl2a	ovary	testis
foxl2b	ovary	ovary
gsdf	testis	testis
sox9a	testis	testis
wnt4a	ovary	testis

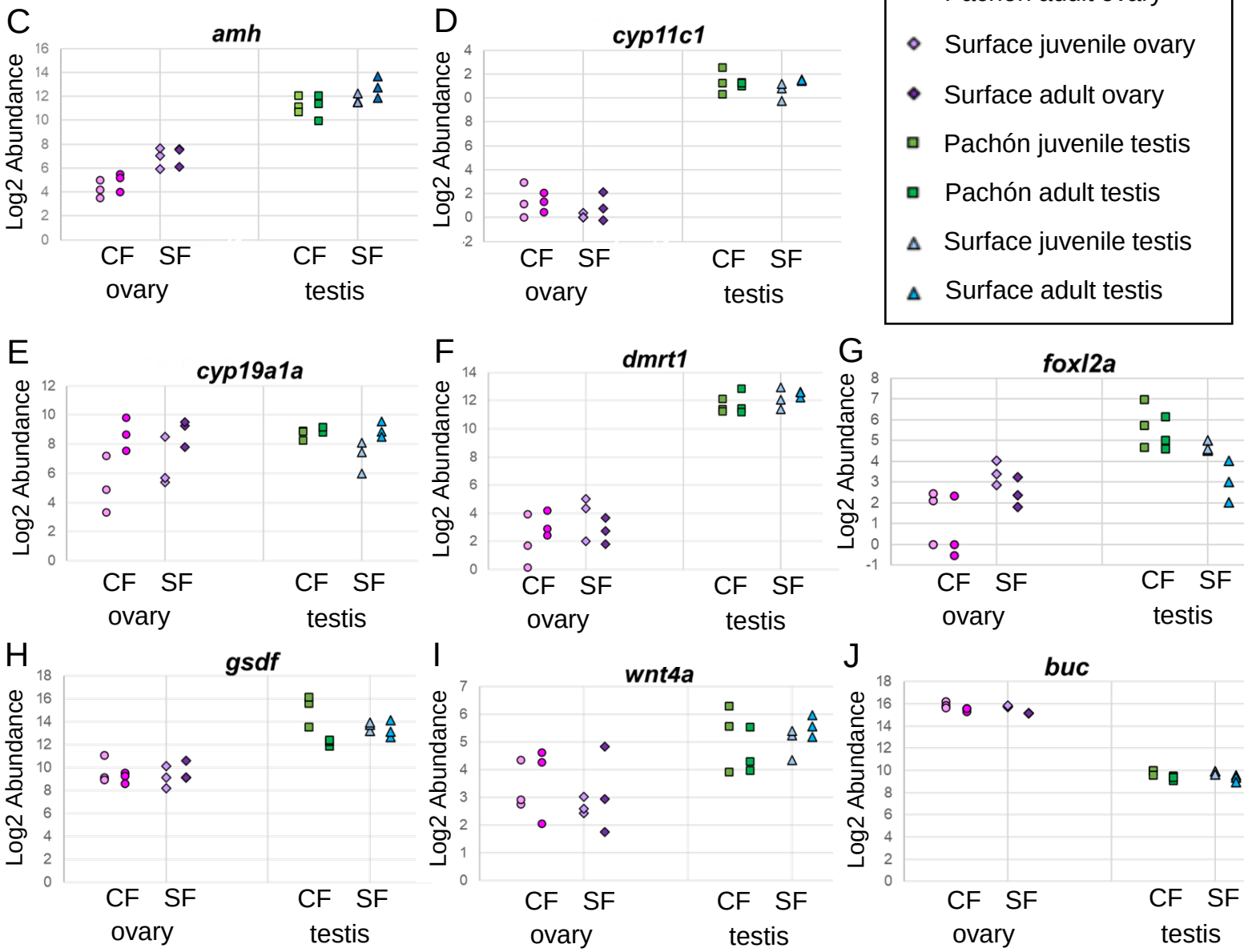

Figure 2

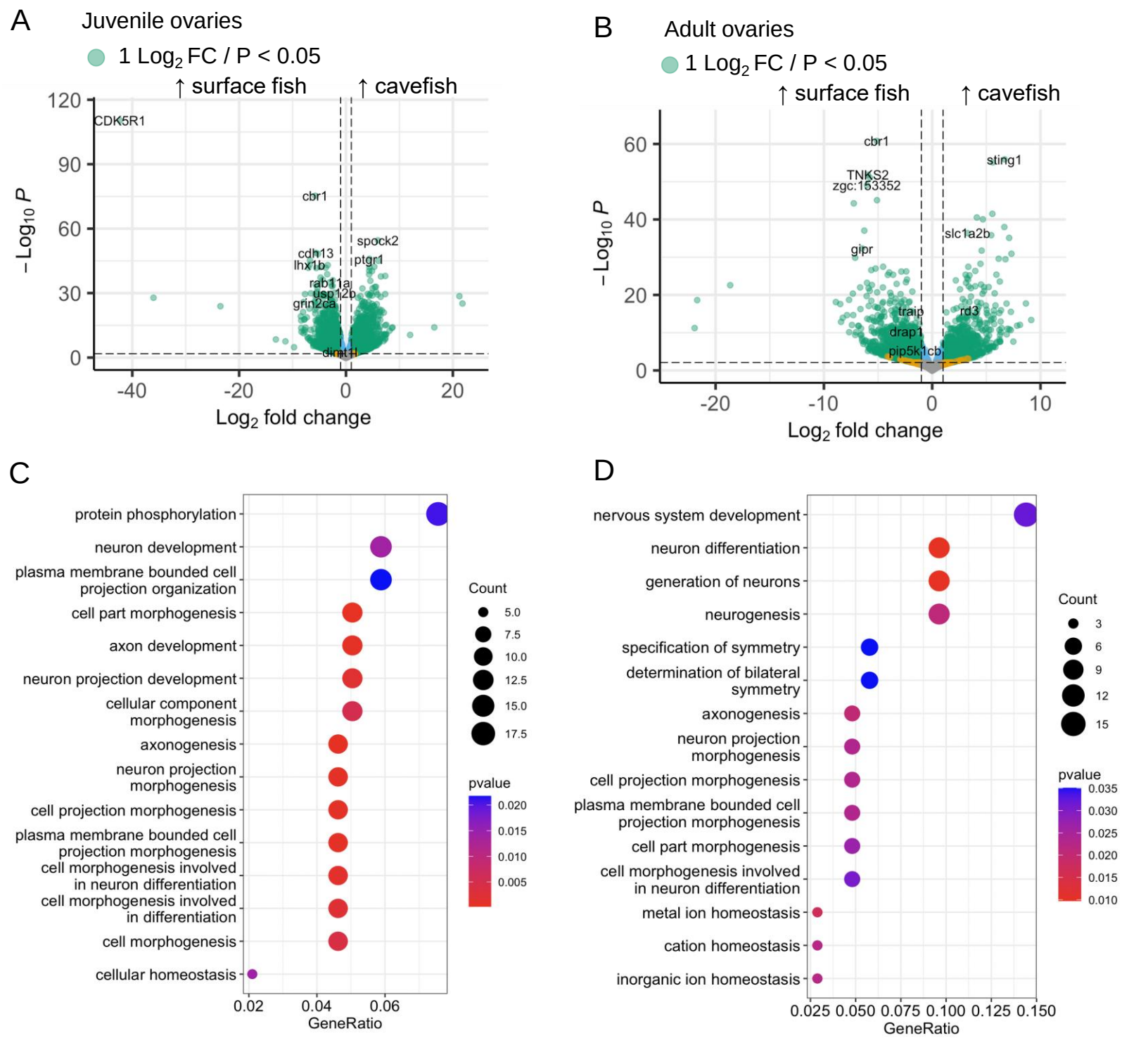
A
Juvenile ovaries
1 Log2 FC / P < 0.05
↑ surface fish
↑ cavefish
CDK5R1
cbr1
cdh13
lhx1b
spock2
ptgr1
rab11a
usp12b
grin2ca
dnmt1l
−Log10 P
Log2 fold change
B
Adult ovaries
1 Log2 FC / P < 0.05
↑ surface fish
↑ cavefish
cbr1
TNKS2
zgc:153352
sting1
slc1a2b
gipr
traip
rd3
drap1
pip5k1cb
−Log10 P
Log2 fold change
C
protein phosphorylation
neuron development
plasma membrane bounded cell projection organization
cell part morphogenesis
axon development
neuron projection development
cellular component morphogenesis
axonogenesis
neuron projection morphogenesis
cell projection morphogenesis
plasma membrane bounded cell projection morphogenesis
cell morphogenesis involved in neuron differentiation
cell morphogenesis involved in differentiation
cell morphogenesis
cellular homeostasis
GeneRatio
Count
pvalue
D
nervous system development
neuron differentiation
generation of neurons
neurogenesis
specification of symmetry
determination of bilateral symmetry
axonogenesis
neuron projection morphogenesis
cell projection morphogenesis
plasma membrane bounded cell projection morphogenesis
cell part morphogenesis
cell morphogenesis involved in neuron differentiation
metal ion homeostasis
cation homeostasis
inorganic ion homeostasis
GeneRatio
Count
pvalue

Figure 3

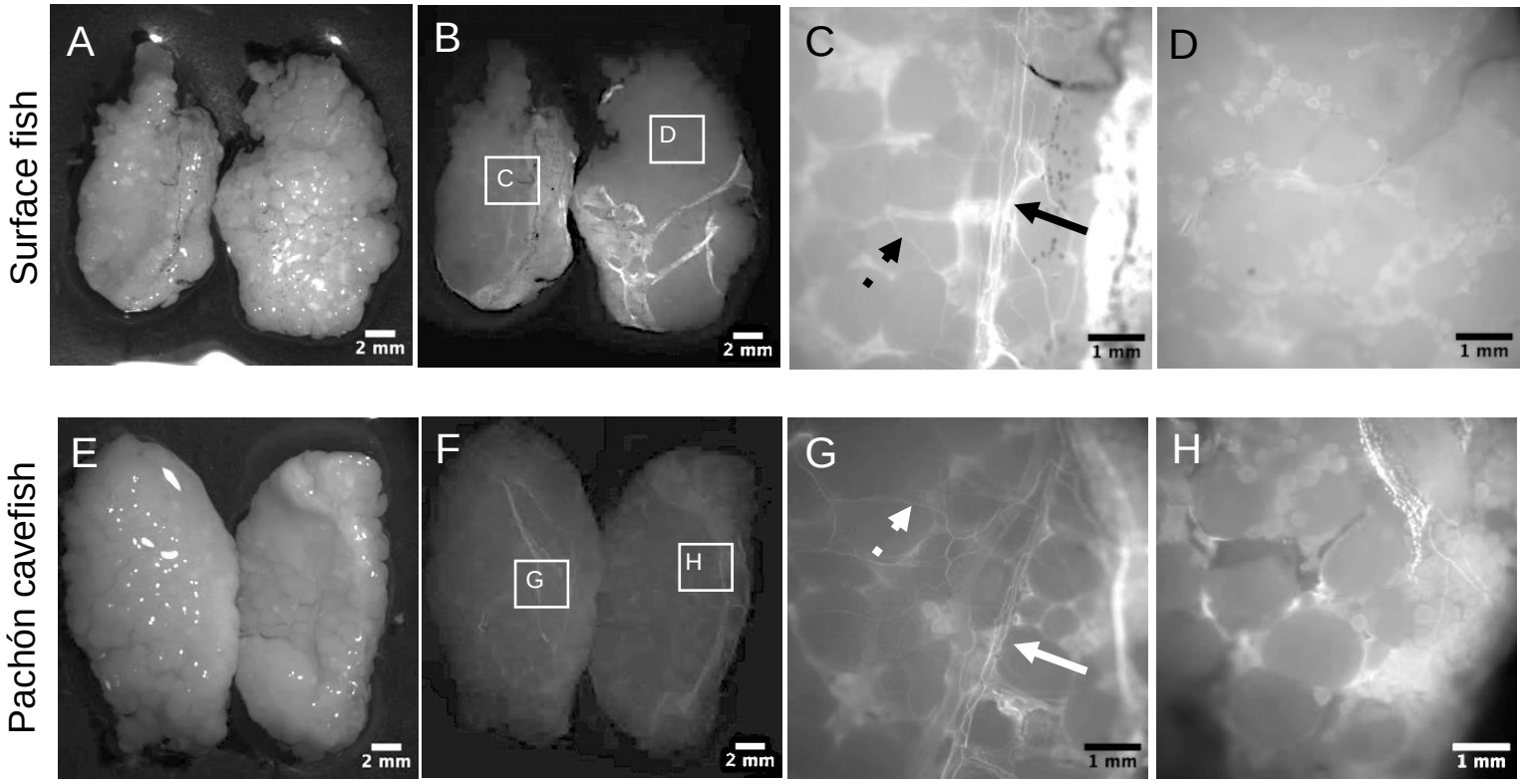

Figure 4

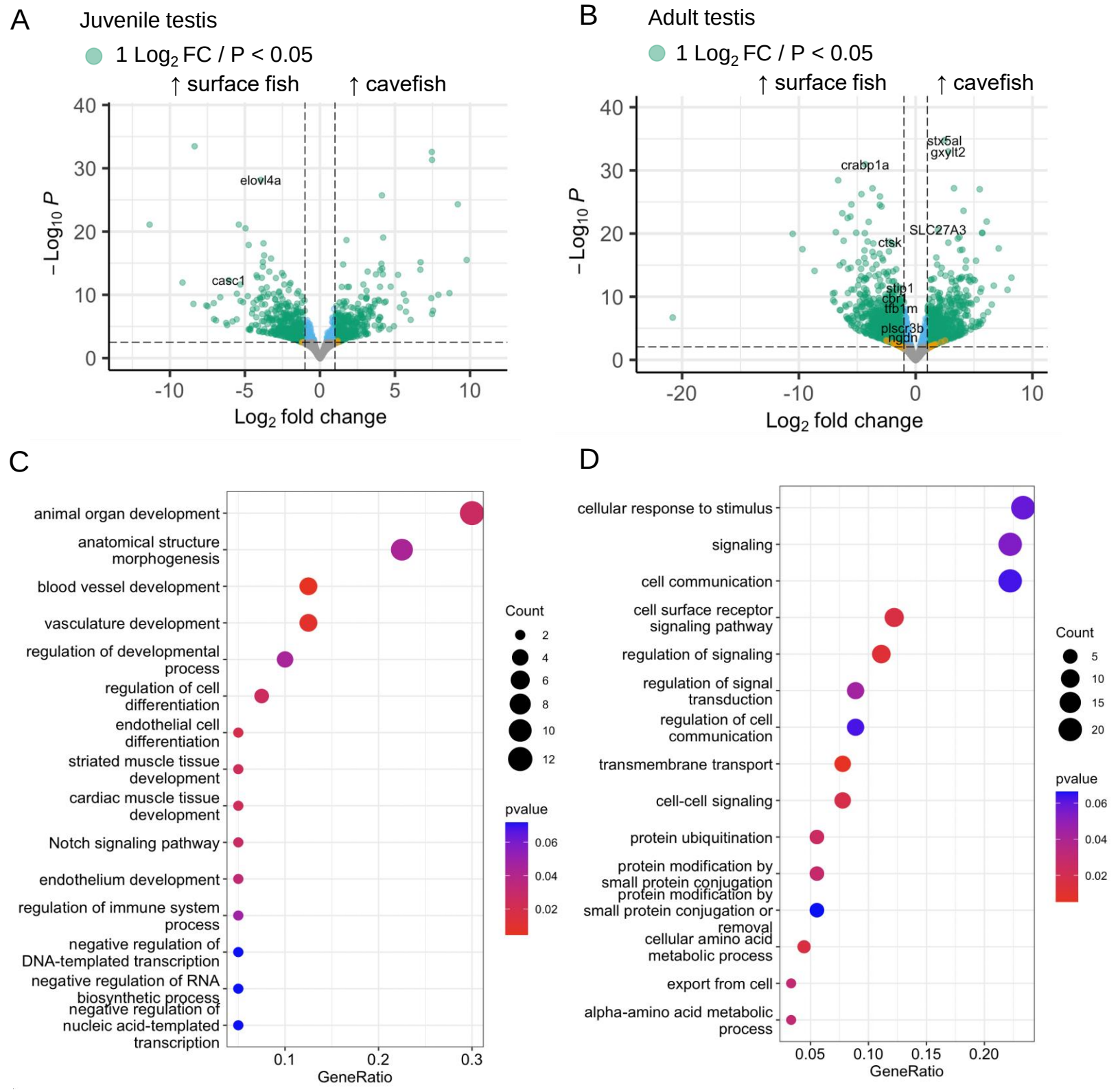
A
Juvenile testis
1 Log2 FC / P < 0.05
↑ surface fish
↑ cavefish
elovl4a
casc1
−Log10 P
Log2 fold change
B
Adult testis
1 Log2 FC / P < 0.05
↑ surface fish
↑ cavefish
crabp1a
stx5al
gxylt2
SLC27A3
ctsk
stip1
cbr1
tfb1m
plscr3b
ngdn
−Log10 P
Log2 fold change
C
animal organ development
anatomical structure morphogenesis
blood vessel development
vasculature development
regulation of developmental process
regulation of cell differentiation
endothelial cell differentiation
striated muscle tissue development
cardiac muscle tissue development
Notch signaling pathway
endothelium development
regulation of immune system process
negative regulation of DNA-templated transcription
negative regulation of RNA biosynthetic process
negative regulation of nucleic acid-templated transcription
GeneRatio
Count
pvalue
D
cellular response to stimulus
signaling
cell communication
cell surface receptor signaling pathway
regulation of signaling
regulation of signal transduction
regulation of cell communication
transmembrane transport
cell-cell signaling
protein ubiquitination
protein modification by small protein conjugation
protein modification by small protein conjugation or removal
cellular amino acid metabolic process
export from cell
alpha-amino acid metabolic process
GeneRatio
Count
pvalue

Figure 5

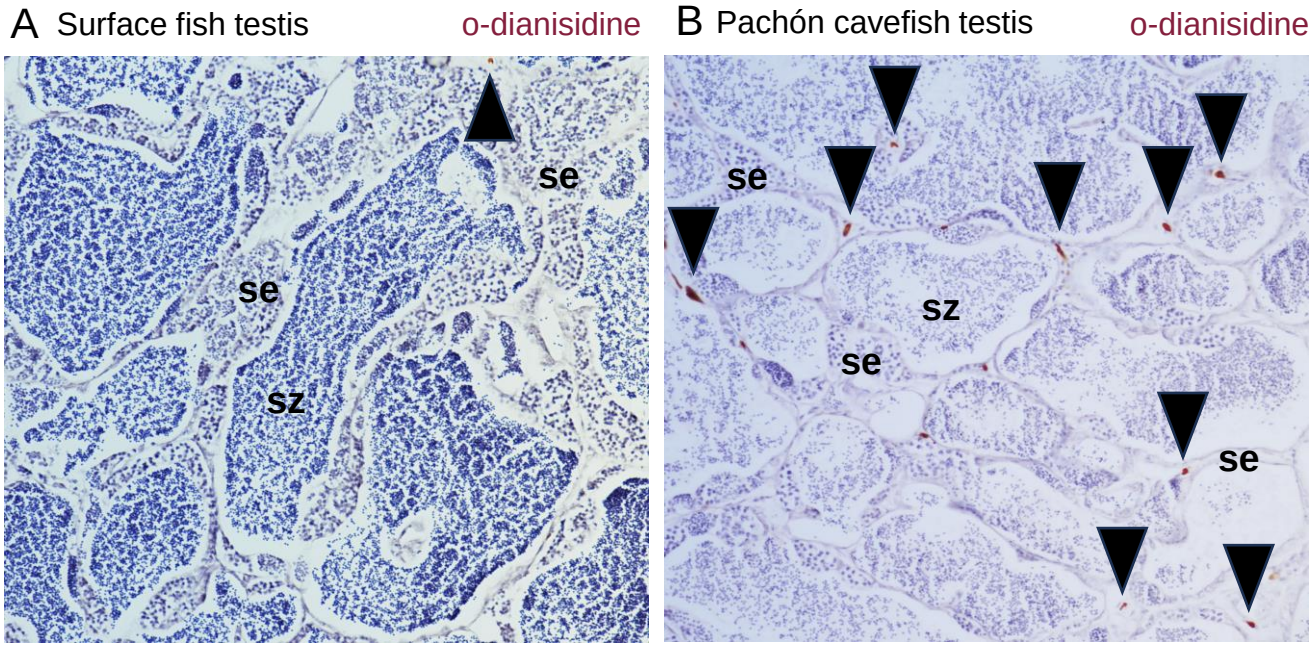
A Surface fish testis
o-dianisidine
se
se
sz
B Pachón cavefish testis
o-dianisidine
se
sz
se
se

Figure 6